DALTON
FULL PAPER

Syntheses, crystal structures, and magnetic properties of first row transition metal coordination polymers containing dicyanamide and 4,4′-bipyridine †

Paul Jensen, Stuart R. Batten, Boujemaa Moubaraki and Keith S. Murray *

School of Chemistry, P.O. Box 23, Monash University 3800, Vic, 3800, Australia.
E-mail: Keith.S.Murray@sci.monash.edu.au

Received 23rd May 2002, Accepted 18th July 2002
First published as an Advance Article on the web 23rd August 2002

The complexes of formulae $M(dca)_2(bipy)$ (M = Fe **1**, Co **2**, Ni **3**; dca = dicyanamide, $N(CN)_2^-$; bipy = 4,4′-bipyridine) and $M(dca)_2(bipy)(H_2O)\cdot 0.5MeOH$ (M = Mn **4**, Fe **5**, Co **6**), have been synthesized and characterized by single crystal and powder X-ray diffraction. Compounds **1**–**3** contain two interpenetrating 3D α-Po related networks. Bidentate dca ligands bridge the octahedral metal atoms to form square-grid like $M(dca)_2$ sheets, with the bipyridine ligands linking these sheets together to form the α-Po-like 3D networks. The large amount of space within a single 3D network allows the interpenetration of the second 3D network. Compounds **4**–**6** contain 1D 'tubes' packing together in a parallel interdigitated fashion. Water ligands coordinated to the octahedral metal ions and intercalated methanol molecules occupy the inside of the $M(dca)_2$ tubes while protruding monodentate bipyridine ligands participate in both π-stacking and hydrogen bonding interactions between adjacent tubes. $Co(dca)_2(bipy)\cdot 0.5H_2O\cdot 0.5MeOH$ **7** and $Cu(dca)_2(bipy)\cdot H_2O$ **8** consist of inclined interpenetrating 2D sheets of $M(dca)_2(bipy)$, while $Cu(dca)_2(bipy)\cdot MeOH$ **9** and $Cu(dca)_2(bipy)\cdot 2H_2O$ **10** contain 2D zigzag sheets of $Cu(dca)_2(bipy)$ with parallel packing. $Fe(dca)_2(bipy)(H_2O)_2\cdot(bipy)$ **11** contains 1D chains of Fe(bipy) with hydrogen bonding extending the topology to that of two 3D interpenetrating α-Po related networks. Compounds **7** and **11** contain octahedral metal ions, while **8** and **9** have five-coordinate Cu atoms. Variable temperature magnetic susceptibility studies (2–300 K; $H = 1$ T) have shown that these framework compounds generally display very weak antiferromagnetic coupling because of the long bipy and $\mu_{1,5}$ bridging pathways. Consequently no long-range magnetic order occurs.

Introduction

The present study of ternary ('linked') complexes formed between divalent d-block metal ions, dicyanamide (dca, $N(CN)_2^-$) and 4,4′-bipyridine (bipy) is part of a wide investigation of molecule-based magnetic materials involving the dca bridging ligand.[1,2] It complements our related work using pyrazine as the linking ligand in which extended framework structures were observed sometimes, as in the present study, involving interpenetration of networks.[3] Our emphasis has been to try to relate structural features to magnetic properties in these coordination polymers. A key aim has been to make new long-range ordered species, as was successfully done in the parent α-$M(dca)_2$ phases[2] and in M(dca)(tcm), where tcm = $C(CN)_3^-$.[4] Magnetic order has, to date, usually required strong magnetic coupling provided by $\mu_{1,3}$ bridging involving the amide N atom of dca. This bridging mode is absent in the present M/dca/bipy species and, thus, long-range order is not anticipated. Nevertheless, the structural features are very interesting. Other groups have studied a number of coordination polymers containing 4,4′-bipyridine from the perspective of porosity and solvent sorption/desorption 'zeolite-like' properties,[5] a feature noted here in terms of intercalation of solvent molecules, often hydrogen bonded to the M/dca/bipy moiety, but not studied in detail.

Experimental

Syntheses

$Fe(dca)_2(bipy)$ 1. A hot (*ca.* 90 °C) aqueous solution (6 ml) of $Fe(BF_4)_2\cdot 6H_2O$ (265 mg, 0.79 mmol) was added to a hot (*ca.* 90 °C) aqueous solution (10 ml) of Na(dca) (100 mg, 1.12 mmol) and 4,4′-bipyridine (90 mg, 0.58 mmol). Fine orange needles formed on cooling (100 mg, 52%). (The sample also contained a few larger red crystals of $Fe(dca)_2(bipy)(H_2O)_2\cdot(bipy)$ which were easily separated.) υ_{max}/cm^{-1} 3620vw, 3382vw, 3069vw, 2320s, 2246m, 2182s, 1606m, 1538w, 1491w, 1413w, 1382m, 1222w, 1069w, 1046vw, 1008vw, 923vw, 815m, 731vw, 668vw, 632w (Nujol). Anal. Calcd for $C_{14}H_8FeN_8$: C, 48.9; H, 2.3; N, 32.6. Found: C, 49.2; H, 2.2; N, 32.8%.

$Co(dca)_2(bipy)$ 2. A warm (*ca.* 50 °C) methanolic solution (8 ml) of Na(dca) (100 mg, 1.12 mmol) and 4,4′-bipyridine (88 mg, 0.56 mmol) was added to a warm (*ca.* 50 °C) aqueous solution (6 ml) of $Co(NO_3)_2\cdot 6H_2O$ (210 mg, 0.72 mmol). Fine pink needles formed immediately (135 mg, 69%). υ_{max}/cm^{-1} 3628vw, 3388vw, 3071vw, 2322s, 2250m, 2188s, 1608m, 1539w, 1492w, 1413w, 1384m, 1222w, 1070w, 1046vw, 1009vw, 922vw, 816m, 731vw, 668vw, 634w (Nujol). Anal. Calcd for $C_{14}H_8CoN_8$: C, 48.4; H, 2.3; N, 32.3. Found: C, 48.3; H, 2.2; N, 32.4%.

$Ni(dca)_2(bipy)$ 3. A hot (*ca.* 90 °C) aqueous solution (10 ml) of Na(dca) (50 mg, 0.56 mmol) and 4,4′-bipyridine (44 mg, 0.28 mmol) was added to a hot (*ca.* 90 °C) aqueous solution (10 ml) of $Ni(NO_3)_2\cdot 6H_2O$ (115 mg, 0.40 mmol). A light blue microcrystalline powder formed immediately (85 mg, 87%). υ_{max}/cm^{-1} 3631vw, 3374vw, 3071vw, 2324s, 2257m, 2197s, 1609m, 1540w, 1492w, 1413w, 1387m, 1222w, 1070w, 1047vw, 1011vw, 922vw, 817m, 732vw, 636w (Nujol). Anal. Calcd for $C_{14}H_8N_8Ni$: C, 48.5; H, 2.3; N, 32.3. Found: C, 48.4; H, 2.3; N, 32.3%.

$Mn(dca)_2(bipy)(H_2O)\cdot 0.5MeOH$ 4. A warm (*ca.* 50 °C) methanolic solution (6 ml) of Na(dca) (103 mg, 1.16 mmol) and

† Electronic supplementary information (ESI) available: atom numbering diagrams for compounds **1** (123 K and 294 K) and **7**–**11**. See http://www.rsc.org/suppdata/dt/b2/b205007b/

 DOI: 10.1039/b205007b

4,4′-bipyridine (89 mg, 0.57 mmol) was added to a warm (*ca.* 50 °C) aqueous solution (2 ml) of $Mn(NO_3)_2{\cdot}4H_2O$ (171 mg, 0.68 mmol). Colorless needles formed after several hours (105 mg, 49%). υ_{max}/cm^{-1} 3588vw, 3536vw, 3336vw, 3238w, 3084vw, 2414vw, 2305s, 2244m, 2189s, 1647vw, 1602m, 1538w, 1490w, 1413w, 1367m, 1350w, 1322vw, 1220w, 1062w, 1044vw, 1019w, 1004vw, 974vw, 930vw, 810m, 731w, 668vw, 626w (Nujol). Anal. Calcd for $C_{14.5}H_{12}MnN_8O_{1.5}$: C, 46.2; H, 3.2; N, 29.7. Found: C, 46.0; H, 3.1; N, 29.7%.

$Fe(dca)_2(bipy)(H_2O){\cdot}0.5MeOH$ 5. A warm (*ca.* 50 °C) methanolic solution (5 ml) of Na(dca) (100 mg, 1.12 mmol) and 4,4′-bipyridine (89 mg, 0.57 mmol) was added to a warm (*ca.* 50 °C) aqueous solution (4 ml) of $Fe(BF_4)_2{\cdot}6H_2O$ (260 mg, 0.77 mmol). Fine orange needles formed on cooling (95 mg, 45%). υ_{max}/cm^{-1} 3590vw, 3329vw, 3240vw, 3084vw, 2304s, 2246m, 2192s, 1648vw, 1602m, 1538w, 1490vw, 1412w, 1366m, 1348w, 1318vw, 1220w, 1062w, 1045vw, 1019w, 1004vw, 812m, 731vw, 668vw, 627w (Nujol). Anal. Calcd for $C_{14.5}H_{12}FeN_8O_{1.5}$: C, 46.1; H, 3.2; N, 29.6. Found: C, 45.9; H, 2.9; N, 30.1%.

$Co(dca)_2(bipy)(H_2O){\cdot}0.5MeOH$ 6. $Co(NO_3)_2{\cdot}6H_2O$ (93 mg, 0.32 mmol) was placed in a 2 cm tube and layered with water (10 ml) with the solid dissolving in the first few millilitres of water. This was then carefully layered with methanol (15 ml) followed by a methanolic solution (10 ml) of Na(dca) (50 mg, 0.56 mmol) and 4,4′-bipyridine (44 mg, 0.28 mmol) and the reaction mixture stoppered. Fine pink needles of **2** formed after several days and provided the crystal for the structure determination of **2**. Several months later almost all needles of **2** had disappeared leaving well formed large red crystals of **6** (55 mg, 51%). υ_{max}/cm^{-1} 3602vw, 3521vw, 3322vvw, 3242w, 3087vw, 2407vw, 2306s, 2250m, 2195s, 1648vw, 1602m, 1538w, 1489w, 1412w, 1367m, 1347w, 1322vw, 1219w, 1062w, 1044vw, 1020w, 1004vw, 926vw, 812m, 732w, 668vw, 656vw, 628w (Nujol). Anal. Calcd for $C_{14.5}H_{12}CoN_8O_{1.5}$: C, 45.7; H, 3.2; N, 29.4. Found: C, 45.8; H, 3.0; N, 29.7%.

$Co(dca)_2(bipy){\cdot}0.5H_2O{\cdot}0.5MeOH$ 7. A few orange crystals (*ca.* 2 mg) were found clustered together in the slow diffusion reaction that eventually formed **6**. When these were found the reaction contained mostly needles of **2**.

$Cu(dca)_2(bipy){\cdot}H_2O$ 8. A warm (*ca.* 50 °C) methanolic solution (7 ml) of Na(dca) (100 mg, 1.12 mmol) and 4,4′-bipyridine (90 mg, 0.57 mmol) was added to a warm (*ca.* 50 °C) aqueous solution (6 ml) of $Cu(NO_3)_2{\cdot}3H_2O$ (144 mg, 0.60 mmol). A blue/green powder formed immediately (180 mg, 87%). υ_{max}/cm^{-1} 3568vw, 3495vw, 3392vw,br, 3103vw, 3074vw, 3052vw, 2306m, 2283m, 2246m, 2218m, 2166s, 2153s,sh, 1648vw, 1610m, 1537w, 1492w, 1416w, 1364m, 1328vw, 1220w, 1070w, 1044vvw, 1032vvw, 1015vw, 929vw, 913vw, 820m, 726w, 668vvw, 646w (Nujol). Anal. Calcd for $C_{14}H_{10}CuN_8O$: C, 45.5; H, 2.7; N, 30.3. Found: C, 46.5; H, 2.2; N, 31.1%. Analysis indicated loss of water (Anal. Calcd for $C_{14}H_8CuN_8$: C, 47.8; H, 2.3; N, 31.9%).

$Cu(dca)_2(bipy){\cdot}MeOH$ 9. A warm (*ca.* 50 °C) methanolic solution (10 ml) of Na(dca) (100 mg, 1.12 mmol) and 4,4′-bipyridine (89 mg, 0.57 mmol) was added to a warm (*ca.* 50 °C) 50 : 50 aqueous methanol solution (10 ml) of $Cu(NO_3)_2{\cdot}3H_2O$ (150 mg, 0.62 mmol). A green/blue powder formed immediately. The reaction mixture was stoppered and after several weeks most of the powder disappeared, leaving only dark blue crystals. The mixture was shaken, the solvent decanted (with the crystals settled and the powder still suspended), and fresh methanol added. The process was repeated to remove most of the powder from the dark blue crystals (*ca.* 100mg, 47% yield) which were then kept under methanol. These were used in the X-ray crystallographic determination.

$Cu(dca)_2(bipy){\cdot}2H_2O$ 10. A few dark blue crystals (*ca.* 10 mg) were separated by eye from a mixture formed in a slow diffusion of $Cu(NO_3)_2{\cdot}3H_2O$, Na(dca), and 4,4′-bipyridine in water/methanol. These were then stored under methanol since they were initially believed to be crystals of **9**. υ_{max}/cm^{-1} 3586vvw, 3396w, 3081vw, 3054vw, 2307m, 2295m, 2243m, 2195sh, 2177s, 1652vw, 1612m, 1537w, 1488w, 1418w, 1375m, 1357w, 1321w, 1218w, 1080w, 1023w, 922vw, 861vw, 823w, 818sh, 731vvw, 668vw, 646vw (Nujol). Anal. Calcd for $C_{14}H_{12}CuN_8O_2$: C, 43.4; H, 3.1; N, 28.9. Found: C, 45.7; H, 2.7; N, 29.4%. Analysis indicated either loss of water (Anal. Calcd for $C_{15}H_{10}CuN_8$: C, 49.3; H, 2.8; N, 30.6%) and/or mixture with **9** (Anal. Calcd for $C_{15}H_{12}CuN_8O$ (**9**): C, 46.9; H, 3.2; N, 29.2%).

$Fe(dca)_2(bipy)(H_2O)_2{\cdot}(bipy)$ 11. A few large red crystals (*ca.* 5 mg) were separated by eye from the preparation of **1**. υ_{max}/cm^{-1} 3227m/br, 3059w, 2284m, 2221m, 2195m, 2160s, 1654vvw, 1648vvw, 1604m, 1537w, 1491vw, 1409w, 1355m, 1318w, 1222w, 1214vw, 1070w, 1061w 1046vw, 1003w, 917vvw, 819w, 807w (Nujol).

X-Ray structural analyses

Single crystal structural analyses for all compounds (except **3**) were performed with a Nonius KappaCCD diffractometer using graphite monochromated Mo-Kα radiation (λ = 0.71073 Å). The data were collected, processed, and corrected for Lorentz and polarization effects using Nonius software.[6] All crystals (except **11**) were face-indexed and numerical absorption corrections applied using the XPREP program[7] or maXus software.[8] Structures were solved and expanded using Fourier techniques within teXsan software,[9] while the final full-matrix least-squares refinements on F^2 were performed with SHELXL-97.[10] Where data were collected at different temperatures, the same crystal was used for each study.

All non-hydrogen atoms were refined anisotropically for **1** and **7**–**11**, except for the disordered solvent molecules in **7** and **8**. Non-hydrogen atoms for **2**, **4**, and **6** were also refined anisotropically, however the thermal parameters for some atoms were fixed to prevent them becoming non-positive definite. For **5** only the metal atoms were refined anisotropically, while thermal parameters for some of the remaining isotropic atoms were fixed. Hydrogen atoms were assigned to calculated positions and were not refined. Hydroxy hydrogen atoms were not assigned except for **9** and **11** where in each case the position of the hydrogen atom was freely refined with a fixed isotropic thermal parameter. In the polar structures of **1** (123 K), **2**, **4**–**6** and **8** the coordinates of some atoms were not refined in order to fix the origin.

1 (293 K) and **8** were refined as racemic, while **1** (123 K), **2**, and **4**–**6** were refined with combined general and racemic twinning. **1** (123 K) and **2** were refined with four components (TWIN 1 0 0 0 −1 0 0 0 −1 −4) while **4**–**6** were refined with two components (TWIN 0 −1 0 −1 0 0 0 0 1). In the latter case the two components are opposite enantiomers that are related by a combination of the general twin law and inversion. Various constraints and restraints on **4**–**6** were used to obtain stable refinements for each of these structures and to prevent unacceptable bond lengths and thermal parameters. Further crystallographic details are given in Tables 1 and 2.

CCDC reference numbers are 172403 (**1**, 123 K), 172404 (**1**, 293 K), 172405 (**2**), and 172406–172413 (**4**–**11**).

See http://www.rsc.org/suppdata/dt/b2/b205007b/ for crystallographic data in CIF or other electronic format.

Powder X-ray diffraction data were collected at room temperature on bulk samples with a Scintag automated powder diffractometer using Cu-Kα radiation (λ = 1.54059 Å). The programs CrystalDiffract[11] and UnitCell[12] were used to refine unit cells, using appropriate known cells as starting

Table 1 Crystallographic data for **1**, **2** and **4**–**6**

	1	**1**	**2**	**4**	**5**	**6**
T/K	123(2)	293(2)	123(2)	293(2)	123(2)	123(2)
Formula	$FeC_{14}H_8N_8$	$FeC_{14}H_8N_8$	$CoC_{14}H_8N_8$	$Mn_2C_{29}H_{24}N_{16}O_3$	$Fe_2C_{29}H_{24}N_{16}O_3$	$Co_2C_{29}H_{24}N_{16}O_3$
M	344.13	344.13	347.21	754.52	756.34	762.50
Crystal system	Monoclinic	Orthorhombic	Monoclinic	Tetragonal	Tetragonal	Tetragonal
Space group	*Pn*	*Pmn*21	*Pn*	$P4_1$	$P4_1$	$P4_1$
a/Å	8.6367(2)	11.5198(2)	8.5824(3)	22.5468(3)	22.3171(4)	22.2246(2)
b/Å	16.8457(4)	17.0112(4)	16.7687(7)	22.5468(3)	22.3171(4)	22.2246(2)
c/Å	11.5033(2)	8.6659(2)	11.4092(4)	13.4343(1)	13.2602(1)	13.1576(1)
α/°	90	90	90	90	90	90
β/°	90.010(2)	90	90.068(3)	90	90	90
γ/°	90	90	90	90	90	90
U/Å^3	1673.63(6)	1698.22(6)	1641.96(11)	6829.44(14)	6604.28(17)	6498.97(10)
Z	4	4	4	8	8	8
D_{calc}/g cm^{-3}	1.366	1.346	1.405	1.468	1.521	1.559
μ(Mo-Kα)/mm^{-1}	0.911	0.898	1.056	0.797	0.938	1.081
F(000)	696	696	700	3072	3088	3104
Data collected	25078	25510	11937	87307	60593	62963
Unique data (Rint)	7574 (0.0314)	4219 (0.0477)	7735 (0.0540)	18370 (0.0632)	15206 (0.0990)	16005 (0.0399)
Observed data [$I>2\sigma(I)$]	6697	3131	4881	10512	10154	13230
Final $R1$, wR_2 [$I>2\sigma(I)$][a]	0.0315, 0.0674	0.0382, 0.0852	0.0606, 0.0824	0.0488, 0.0951	0.0730, 0.1237	0.0335, 0.0730
R_1, wR_2 (all data)	0.0406, 0.0711	0.0653, 0.0966	0.1218, 0.0967	0.1148, 0.1169	0.1239, 0.1420	0.0504, 0.0789
Goodness of fit, S	1.030	1.029	0.982	0.972	1.028	1.035
$\Delta\rho_{min}$, $\Delta\rho_{max}$/e Å^{-3}	−0.387 /0.465	−0.348 /0.430	−0.605 /0.467	−0.565 /0.361	−0.562 /0.722	−0.574 /0.523

[a] $R_1 = \Sigma||F_o| - |F_c||/\Sigma|F_o|$, $wR_2 = [\Sigma w(F_o^2 - F_c^2)^2/\Sigma w(F_o^2)^2]^{1/2}$.

Table 2 Crystallographic data for **7**–**11**

Compound	**7**	**8**	**9**	**10**	**11**
T/K	123(2)	173(2)	173(2)	173(2)	123(2)
Formula	$CoC_{14.5}H_{11}N_8O$	$CuC_{14}H_{10}N_8O$	$CuC_{15}H_{12}N_8O$	$CuC_{14}H_{12}N_8O_2$	$FeC_{24}H_{20}N_{10}O_2$
M	372.24	369.84	383.87	387.86	536.35
Crystal system	Orthorhombic	Orthorhombic	Monoclinic	Monoclinic	Triclinic
Space group	*Pccn*	$Pna2_1$	$P2_1/c$	$P2_1/c$	$P\bar{1}$
a/Å	11.6750(4)	7.3887(4)	8.6253(2)	8.3713(5)	8.1365(1)
b/Å	19.4612(5)	11.9610(6)	12.5777(3)	13.0693(6)	8.6926(1)
c/Å	7.3249(3)	18.7679(10)	14.8959(4)	15.0030(9)	9.7297(2)
α/°	90	90	90	90	102.531(1)
β/°	90	90	93.421(1)	92.033(3)	107.798(1)
γ/°	90	90	90	90	97.420(1)
U/Å^3	1664.29(10)	1658.64(15)	1613.12(7)	1640.40(16)	625.31(2)
Z	4	4	4	4	1
D_{calc}/g cm^{-3}	1.486	1.481	1.581	1.570	1.424
μ(Mo-Kα)/mm^{-1}	1.051	1.335	1.376	1.358	0.646
F(000)	756	748	780	788	276
Data collected	15388	11369	23470	14570	10573
Unique data (Rint)	2518 (0.037)	4235 (0.0343)	4456 (0.0358)	3955 (0.0491)	3031 (0.023)
Observed data [$I>2\sigma(I)$]	1714	3130	3741	2906	2743
Final R_1, wR_2 [$I>2\sigma(I)$][a]	0.0384, 0.0966	0.0458, 0.1104	0.0325, 0.0838	0.0450, 0.1032	0.0318, 0.0704
R_1, wR_2 (all data)	0.0685, 0.1089	0.0742, 0.1217	0.0430, 0.0891	0.0718, 0.1136	0.0376, 0.0727
Goodness of fit, S	1.047	1.051	1.041	1.057	1.036
$\Delta\rho_{min}$, $\Delta\rho_{max}$/e Å^{-3}	−0.597 /0.520	−0.537 /0.395	−0.594 /0.430	−0.553 /0.646	−0.305 /0.278

[a] $R_1 = \Sigma||F_o| - |F_c||/\Sigma|F_o|$, $wR2 = [\Sigma w(F_o^2 - F_c^2)^2/\Sigma w(F_o^2)^2]^{1/2}$.

points, to confirm that single crystals were representative of bulk samples.

Magnetic measurements

Magnetic measurements were made using a Quantum Design MPMS 5 SQUID magnetometer with an applied field of 1 T. The powdered samples were contained in a gelatin capsule that was held in the centre of a drinking straw and fixed to the end of the sample rod. Measurements of the magnetisation, with field cooling (FCM) and zero-field cooling (ZFCM), in an applied field of 5 Oe were carried out to test for the presence of long-range magnetic order. Single crystal measurements of $\chi_{||}$ and $\chi_{\perp}$ for the Co(II) complex **6** were made in a longitudinal field with the crystal fixed by shellac to a flat face ground on a 2 mm Perspex sample rod. Two crystals were used, one with H parallel to c ($\chi_{||}$), and one with H parallel to a ($\chi_{\perp}$).

Results and discussion

Synthesis and characterisation

Reaction of sodium dicyanamide, 4,4′-bipyridine, and transition metal salts in water or aqueous alcohol in the mole ratio of 2 : 1 : 1 leads to the formation of coordination polymers of general formula $M(dca)_2(bipy)$. Different structures are possible depending on both the preference of the metal ion used and inclusion of coordinated and/or intercalated solvent molecules. Synthesis from hot water favours formation of unsolvated $M(dca)_2(bipy)$ for M = Fe, Co, and Ni, while synthesis from aqueous methanol can lead to mixtures that include solvated $M(dca)_2(bipy)(H_2O)\cdot 0.5MeOH$. Methanol appears to be necessary for formation of these solvated networks. In the case of Mn(II), however, the solvated network is the favoured product and forms in both the presence and absence of methanol. In the latter case the formula is $Mn(dca)_2(bipy)(H_2O)\cdot 0.5H_2O$ and the

structure, which contains intercalated water molecules instead of methanol, was recently reported by Manson *et al.*[13]

X-Ray powder diffraction was necessary with bulk microcrystalline samples to confirm the presence of a single phase. Highly crystalline samples were obtained by either slow diffusion of reagents or slow cooling of relatively dilute hot reaction mixtures. In these cases it was often possible to visually identify multiple phases and obtain a single crystal structure on each. Slow diffusion reactions were performed by layering methanol solutions of sodium dicyanamide and 4,4′-bipyridine on top of aqueous solutions of the metal salts. One such reaction provided the source for all three Co(II) structures. Initially, fine pink needles of **2** formed as the reagents slowly mixed. Weeks later a very small cluster of orange crystals of **7** were found in one area of the reaction vessel, and several months later almost all of these two phases had disappeared leaving beautiful red crystals of **5**. A similar reaction with Cu(II) initially yielded mainly well formed green/blue needles of **8** and also a small amount of very small green prisms (yet to be characterised). After a few days large dark blue prisms of **9** also formed. In another reaction with Cu(II) these dark blue prisms appeared less intense in colour and were found to be that of **10**. The only difference between these two blue compounds is that each intercalated methanol in **9** is replaced with two intercalated water molecules in **10**.

These reactions have shown that several different structures can be obtained from the reagents in the ratio used.[14] Some compounds are difficult to obtain free from contaminants and require further refinement of synthetic methods. Samples of **6**, **9**, and **10** used for magnetic or elemental analyses were obtained only after physical separation from other compounds. The highly crystalline sample of **1** also contained a small cluster of red crystals of **11** ($Fe(dca)_2(bipy)(H_2O)_2\cdot(bipy)$) indicating that compounds with other M : dca : bipy stoichiometries can also form in these reactions. This was easily separated by eye.

The compounds give well resolved infrared spectra with characteristic peaks present from dicyanamide and 4,4′-bipyridine. Solvated species also gave the characteristic ν(OH) bands in the 3200–3400 cm^{-1} region, although rather weak in comparison to the nitrile stretches. The spectra for the five-coordinate Cu compounds **8**–**10** contained splitting of the peaks in the nitrile stretching region indicative of the presence of both monodentate and bidentate dicyanamide.

X-Ray crystallography

Compounds **1** and **2** are similar to the topologically related α-$M(dca)_2(pyz)$ series[3] {pyz = pyrazine} in that they undergo a phase change upon cooling which simultaneously induces twinning of the crystals. In both systems the dca ligands in the high temperature phase are disordered about a mirror plane. Below the phase change temperature they become ordered and the mirror plane symmetry is lost. Separate domains within each crystal order differently resulting in pseudo-merohedral twinning. The phase change in both systems is from orthorhombic to monoclinic symmetry, however the space groups in each case are different. The pyrazine systems are centrosymmetric and change from *Pnma* to $P2_1/n$, while the 4,4′-bipyridine systems are non-centrosymmetric and change from $Pmn2_1$ to *Pn*. Analysis of the *hk*0 reflections for the pyrazine systems distinguishes between the *Pnma* and $P2_1/n$ space groups. For the bipyridine series, however, $Pmn2_1$ and *Pn* have the same systematic absences and the correct assignment is based on the quality of the solution and refinement. The 4,4′-bipyridine structures are also racemically twinned. Hence **1**, at 293 K, was refined in $Pmn2_1$ using the racemic twin law {−1 0 0, 0 −1 0, 0 0 −1} with the twin component refining close to 0.5. The low temperature solutions (**1** at 123 K, and **2**) were refined with combined general twinning (twin law same as above) and racemic twinning.

A disordered solution for **2** was published recently by Sun *et al.*[15] Data were collected at 293 K, and the solution refined in *Pnma*. This solution is most probably incorrect, since it contains both disordered bipy and dca moieties. The dca ligands are disordered about the mirror plane while the bipy rings are positionally disordered. The apparent disorder of the bipy ligands is most likely due to incorrect space group selection and is imposed by the centricity of *Pnma*. Our solution of **1** at the same temperature (293 K) in $Pmn2_1$ shows no disorder of the bipy ligands and we would not expect to see anything different for **2**. Examination of the systematic absences for these systems shows that *hk*0 and 0*k*0 reflections are present for $k \neq 2n$ ($Pmn2_1$ orientation), although they are very weak. This can lead to incorrect assignment of *Pnma* when using automatic space group selection programs. In fact, this actually occurred with our initial solution of **2** (123 K), which gave disordered bipy and dca molecules, high *R* values and poor thermal parameters.

The structures of **4**–**6** were solved in the chiral tetragonal space group $P4_1$. Initial solutions were poor until refined using the twin law {0 −1 0, −1 0 0, 0 0 1}. The data for solutions for **5** and **6** were collected at 123 K while the solution for the isostructural complex **4** was obtained at 293 K. The room temperature data for **4** was collected after problems with the low temperature (123 K) solution. At 123 K, **4** is not tetragonal but appears to be orthorhombic due to the difference in cell dimensions for *a* and *b* when refined freely during data processing. A suitable refinement for this low temperature solution has not yet been finalised due to twinning problems. The mosaicity for **4** is higher at low temperature compared to room temperature and this is consistent with the presence of pseudo-merohedral twinning occurring at low temperature as was observed for **1**. A structure solution for the closely related compound $Mn(dca)_2(bipy)(H_2O)\cdot0.5H_2O$ appeared recently.[13] This was refined in orthorhombic *Iba*2 with disordered water molecules. *Iba*2 is not the correct space group for **4** since the data are primitive, however it is noted that the data are weak for $h + k + l \neq 2n$ as is the case for all of **4**–**6**, indicating that the structures are pseudo-*I*-centred. Our tetragonal solutions show that all the solvent molecules in the structures are ordered. It is possible that if data were collected using a point detector that the weak data could be missed and the *I*-centred cell determined incorrectly, however with a CCD detector such data cannot be overlooked. It is therefore quite possible that the apparent disorder of solvent molecules arises from the symmetry of an incorrect space group as was similarly noted for **2**. The correct solution for **4** at 123 K is probably primitive orthorhombic (chiral) with combined pseudo-merohedral and racemic twinning.

Structures

The structures show a variety of topologies and dimensionalities. Compounds **1**–**3** contain two interpenetrating α-Po-related[16] 3D networks. In contrast, compounds **4**–**6** contain unusual 1D tube-like networks. Compounds **7**–**10** contain 2D (4,4) networks[16] which display inclined interpenetration[16] in **7** and **8**. The structure of **11** contains 1D coordination chains which are linked by hydrogen bonding interactions into two interpenetrating α-Po-related networks.

This structural variety is partly due to the fact that the two ligands show a range of coordination modes. Compounds **1**–**7** contain bidentate dca ligands, **8**–**10** contain both bidentate and monodentate dca ligands, while compound **11** contains only monodentate dca ligands. The bipy ligand is bidentate in **1**–**3** and **7**–**10**, while in **11** it is both bidentate and uncoordinated (but hydrogen bonding) and in **4**–**6** it is monodentate. Hydrogen bonding interactions feature prominently in **4**–**6** and **9**–**11**, while the metal coordination geometries in all the compounds except **8**–**10** are octahedral. Compounds **8**–**10**, the only structures to contain copper, all contain five-coordinate metal atoms

which each make an additional weak interaction to a sixth donor atom.

M(dca)$_2$(bipy) {1 (M = Fe), 2 (M = Co), and 3 (M = Ni)}. Atom numbering schemes for **1** at 123 K (*Pn*) and at 293 K ($Pmn2_1$) are given in the Supporting Information.† Since **2** is isomorphous with **1** (123 K) the same numbering was used. In both the low and high temperature solutions there are two crystallographically unique metal atoms, four unique dca ligands and two unique bipy ligands. At 293 K, however, only half of each bipy molecule is unique due to the mirror plane symmetry, with each dca ligand disordered about the same mirror plane. The amide nitrogen and carbon atoms of the dca ligands were accordingly refined at half occupancy with the nitrile nitrogens at full occupancy since they reside on the mirror plane.

The metal atoms are octahedral. Each metal atom is connected to four others in the *ab* (*Pn*) or *bc* ($Pmn2_1$) plane by four different dca ligands coordinating *via* the nitrile nitrogens in bidentate bridging mode. This gives square-grid like 2D sheets of M(dca)$_2$ which are connected together in the third dimension by axially coordinating bipy ligands to give an overall α-Po-like[16] network (Fig. 1). The large voids formed by a single 3D

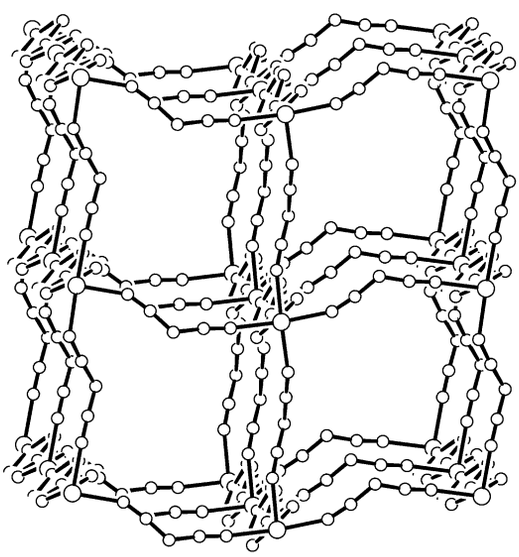

Fig. 1 One of the two interpenetrating 3D α-Po nets in the structure of **2**. Compound **1** is isostructural.

network allow incorporation of a second identical network thus giving two interpenetrating 3D α-Po related networks, as shown in Fig. 2. The aromatic rings in a single network are roughly coplanar with each other but are oriented approximately perpendicular to those of the other network. This situation was observed in the structure of α-Cu(dca)$_2$(pyz) which also had *Pn* symmetry.[3] At 293 K the aromatic rings within each bipy molecule are exactly coplanar with each other since each half is related to the other by the mirror plane of the $Pmn2_1$ space group. At 123 K, however, the mirror plane symmetry is lost and the two rings of each bipy molecule twist slightly with respect to each other.

For **1** (123 K) the Fe–N_{dca} bond lengths range from 2.123(3) to 2.156(3) Å while the Fe–N_{bipy} bond lengths are slightly longer, ranging from 2.187(5) to 2.222(4) Å. Similar trends are observed for **2**. At 293 K, **1** has only two crystallographically unique Fe–N_{bipy} bond lengths {2.204(3) and 2.209(3) Å}, which are equivalent within error, while the corresponding Fe–N_{dca} bond lengths range from 2.113(5) to 2.167(5) Å. The N–M–N bond angles are similar for all three structures and show distortion from true octahedral values. The dca C–N–M bond angles for the low temperature solutions range from 146° to 171°.

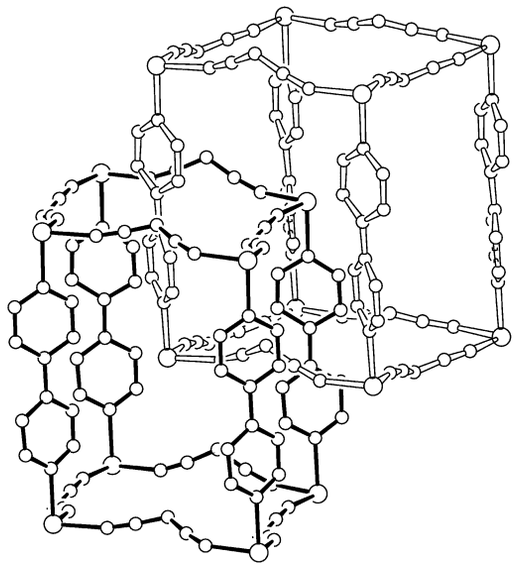

Fig. 2 Two interpenetrating α-Po nets from **2**.

The shortest intranetwork M ··· M distances are along the dicyanamide bridges, being 8.529(1), 8.593(1), and 8.476(2) Å for **1** (123K), **1** (293K), and **2** respectively. The M ··· M distance *via* the 4,4′-bipyridine ligands is *ca.* 11.5 Å. As for the topologically related M(dca)$_2$(pyz) compounds,[3] the shortest M ··· M distance is *between* networks, being 7.924(1), 8.032(1), and 7.886(2) Å respectively for each of **1** (123 K), **1** (293 K), and **2**.

Crystals suitable for single crystal X-ray diffraction could not be obtained for **3**, however powder diffraction (at 293 K) showed that it was isomorphous with **1** (293 K). Refinement of the peak positions gave an orthorhombic cell of a = 11.300(6) Å, b = 16.805(7) Å, c = 8.536(4) Å, U = 1621(1) Å.[3]

M(dca)$_2$(bipy)(H$_2$O)·0.5MeOH {4 (M = Mn), 5 (M = Fe), and 6 (M = Co)}. Atom numbering schemes for the isostructural **4**–**6** are represented by that of **6** shown in Fig. 3. 1D rhombohedral tubes are formed as shown in Fig. 4. Each octahedral metal atom is connected to four others by four different bidentate dca ligands coordinating in the equatorial positions *via* the nitrile nitrogens. The equatorial planes formed by the coordinating nitrile nitrogens lie on the sides of the tubes. Metal atoms on any one side of each tube are separated by the unit cell length c. Metal atoms on opposite sides have approximately the same z coordinates while those on the adjacent sides are displaced from them by approximately c/2. Hence the dca ligands twist around the tubes as viewed down the c axis with the amide nitrogens of the dca ligands forming the edges of the rhombohedral tubes. This contrasts with the square tubes formed in the structure of M(dca)$_2$(apym) {M = Co, Ni, apym = 2-aminopyrimidine}[17] where metal atoms form the edges of the tubes and tridentate dicyanamide ligands lie on the sides.

The axial positions for each metal ion are occupied by a water molecule on the inside of the tube and a monodentate bipy ligand on the outside. The intercalated methanol molecules, along with the coordinated water molecules, occupy the rhombohedral channels formed by the 1D M(dca)$_2$ networks. The methanol molecules appear to template the tube network with both hydrogen bonding and steric interactions with the water molecules. The uncoordinated nitrogen atoms of the protruding monodentate bipy ligands reside at large windows in the sides of adjacent 1D tubes and hydrogen bond to the water molecules inside. These hydrogen bonds extended the overall topology of the structure to two interpenetrating 3D α-Po related networks (Fig. 5). Adjacent 1D coordination networks also interact through interdigitation and π-stacking of the bipy

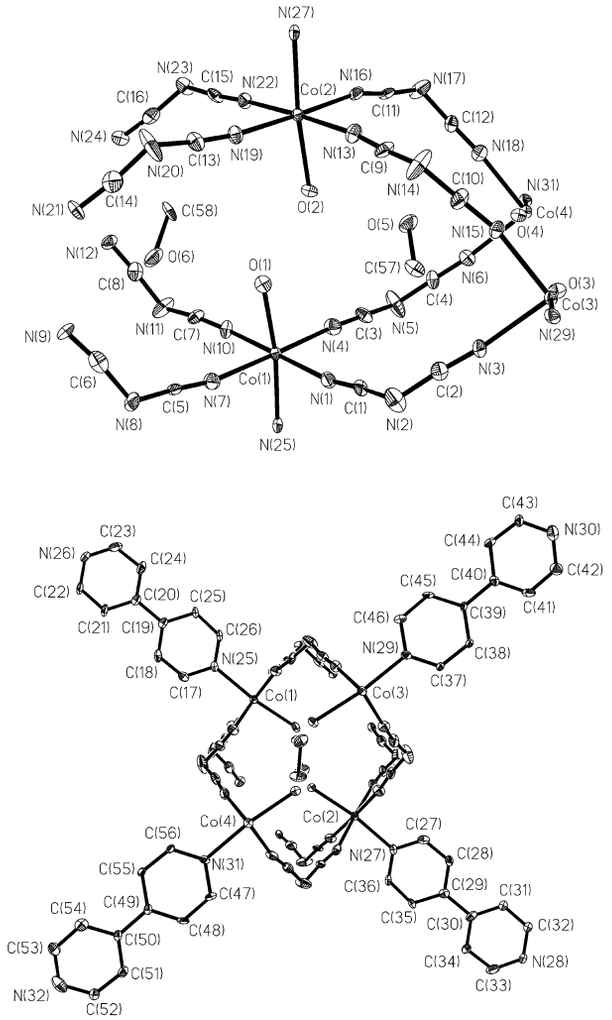

Fig. 3 Atom numbering diagrams for **6**; compounds **4** and **5** have similar numbering schemes.

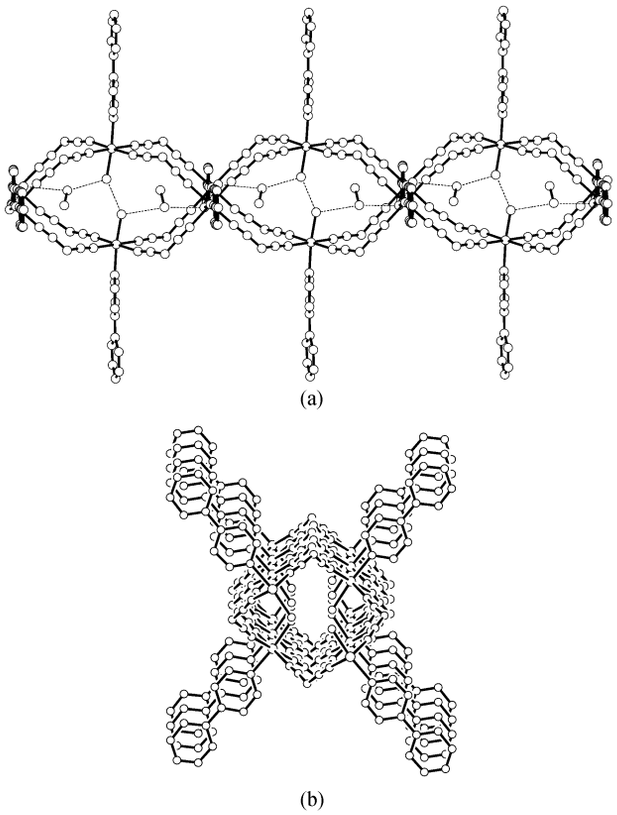

Fig. 4 (a) A side-on view of a 'tube' in the structure of **6**. Note the hydrogen bonding between the intercalated solvent molecules and the coordinated water ligands. (b) A view looking down the axis of the tube.

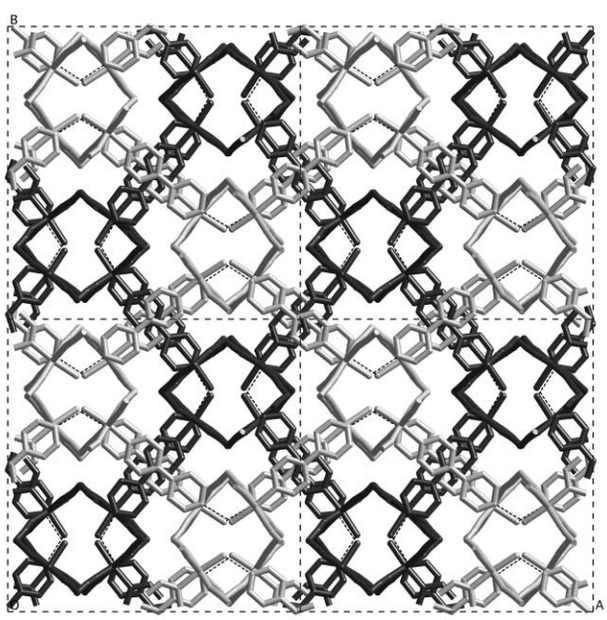

Fig. 5 Packing of tubes in **6**. Hydrogen bonding between the bipy ligands and water ligands of adjacent tubes connect the tubes into two separate networks. These hydrogen bonds are depicted by the dotted lines.

ligands as shown in Fig. 5. Only half of the bipy ligands lie across the 4_1 screw axes that relate the adjacent tubes to each other. The aromatic rings of the bipy ligands appear coplanar for the ligands stacking along the 4_1 axes while in the other columns of stacked bipy ligands the aromatic rings in each molecule are twisted slightly with respect to each other. These columns of bipy ligands lie on pseudo 4_3 screw axes. The slight twisting of the aromatic rings violates 4_3 symmetry as do the positions of the coordinated water molecules, which alternate from below to above the *ab* planes of the metal atoms (*vide infra*).

Selected bond lengths, angles, hydrogen bonding distances, and metal to metal distances for **4**–**6** are listed in Table 3. All metal atoms have very similar octahedral environments, with the axial M–O and $M–N_{bipy}$ bond lengths being slightly longer than the equatorial $M–N_{dca}$ bond lengths.

Metal atoms on opposite sides of the tubes have their coordinated water molecules in close proximity inside the channels. This forces the water molecules to spread away from each other in both the *ab* plane and the *c* direction. In combination with the packing requirements of the protruding bipy ligands, this generates the distortion from octahedral symmetry for the metal ions. The coordinated water molecules are hydrogen bonded together in pairs. The O(1) ··· O(2) and O(3) ··· O(4) distances are equivalent within error and range from 2.805(8) to 2.828(5) Å for all three structures. The methanol molecules in the channels align with their C–O bonds approximately anti-parallel as they alternate down the *c* axis. They reside between and hydrogen bond to the water molecules as shown in Fig. 4(a). O(5) links O(2) to O(4) while O(6) links O(1) to O(3) thus giving order to the hydrogen bond network down each rhombohedral channel. The $O \cdots O_{MeOH}$ hydrogen bond distances range from 2.753(5) to 3.114(9) Å. The methyl groups of the methanol molecules are situated in the voids between coordinated water molecules and also assist in giving order to all molecules in the channels. The $O \cdots N_{bipy}$ hydrogen bond distances are very similar for each structure and

Table 3 Selected bond lengths (Å), angles (°), and distances (Å) for **4**–**6**

	4 (T = 293(2) K)	**5** (T = 123(2) K)	**6** (T = 123(2) K)
M(1)–N(1)	2.217(6)	2.159(7)	2.106(4)
M(1)–N(4)	2.210(6)	2.117(7)	2.087(4)
M(1)–N(7)	2.227(6)	2.187(7)	2.122(4)
M(1)–N(10)	2.224(6)	2.150(7)	2.129(4)
M(1)–N(25)	2.285(5)	2.188(7)	2.145(4)
M(1)–O(1)	2.270(5)	2.214(7)	2.130(3)
M(2)–N(13)	2.196(6)	2.113(7)	2.095(4)
M(2)–N(16)	2.223(7)	2.161(8)	2.092(4)
M(2)–N(19)	2.166(6)	2.109(7)	2.100(4)
M(2)–N(22)	2.232(6)	2.180(8)	2.105(4)
M(2)–N(27)	2.270(6)	2.215(7)	2.155(4)
M(2)–O(2)	2.215(5)	2.173(7)	2.181(3)
M(3)–N(3)	2.221(6)	2.150(7)	2.126(4)
M(3)–N(9)^{i}	2.219(7)	2.155(7)	2.119(4)
M(3)–N(15)	2.180(6)	2.160(7)	2.100(4)
M(3)–N(21)^{i}	2.197(6)	2.167(7)	2.116(4)
M(3)–N(29)	2.257(6)	2.183(7)	2.126(4)
M(3)–O(3)	2.233(5)	2.165(7)	2.188(3)
M(4)–N(6)	2.213(6)	2.175(7)	2.120(4)
M(4)–N(12)^{i}	2.224(7)	2.143(7)	2.104(4)
M(4)–N(18)	2.217(6)	2.121(7)	2.105(4)
M(4)–N(24)^{i}	2.208(6)	2.140(7)	2.133(4)
M(4)–N(31)	2.257(6)	2.172(7)	2.118(4)
M(4)–O(4)	2.254(4)	2.195(6)	2.144(3)
O(1)–M(1)–N(25)	169.3(2)	168.7(3)	170.7(2)
O(2)–M(2)–N(27)	169.2(2)	169.6(3)	171.1(2)
O(3)–M(3)–N(29)	169.9(2)	171.7(3)	171.8(2)
O(4)–M(4)–N(31)	167.8(2)	170.8(3)	171.1(2)
O(1) ··· O(2)	2.828(5)	2.805(8)	2.811(3)
O(3) ··· O(4)	2.828(5)	2.821(8)	2.809(3)
O(6) ··· O(1)	2.786(12)	2.787(9)	2.998(5)
O(6) ··· O(3)^{ii}	3.061(12)	2.984(9)	2.753(5)
O(5) ··· O(2)	3.114(9)	2.931(13)	2.768(5)
O(5) ··· O(4)	2.814(9)	2.835(13)	2.968(5)
O(1) ··· N(30)^{iii}	2.733(7)	2.725(10)	2.761(6)
O(2) ··· N(32)^{iv}	2.704(8)	2.725(11)	2.714(6)
O(3) ··· N(26)^{v}	2.721(8)	2.719(11)	2.714(5)
O(4) ··· N(28)^{vi}	2.744(8)	2.717(11)	2.743(5)
M(1) ··· M(2)	6.560(2)	6.459(2)	6.450(1)
M(3) ··· M(4)	6.566(2)	6.493(2)	6.481(1)
M(1) ··· M(3)	8.191(2)	8.114(2)	8.075(1)
M(1) ··· M(4)	8.349(2)	8.246(2)	8.205(1)
M(1) ··· M(3)^{ii}	7.804(2)	7.666(2)	7.598(1)
M(1) ··· M(4)^{ii}	8.339(2)	8.223(2)	8.170(1)
M(2) ··· M(3)	8.324(2)	8.226(3)	8.189(1)
M(2) ··· M(4)	7.771(2)	7.616(2)	7.557(1)
M(2) ··· M(3)^{ii}	8.344(2)	8.262(3)	8.226(1)
M(2) ··· M(4)^{ii}	8.169(2)	8.080(2)	8.038(1)
M(1) ··· (M1)^{vii}	7.447(2)	7.386(2)	7.349(1)
M(2) ··· M(2)^{viii}	7.465(2)	7.409(2)	7.359(1)
M(3) ··· M(4)^{vii}	7.376(2)	7.288(2)	7.235(1)
M(3) ··· M(4)^{ix}	7.532(2)	7.481(2)	7.441(1)

Symmetry operations:i x, y, $z + 1$; ii x, y, $z - 1$; iii $-x$, $1 - y$, $z - 1/2$; iv $1 - x$, $-y$, $z - 1/2$; v $-x$, $-y$, $z + 1/2$; vi $1 - x$, $1 - y$, $z + 1/2$; vii $-y$, x, $z + 1/4$; viii $1 - y$, x, $z + 1/4$; ix y, $1 - x$, $z - 1/4$.

range from 2.704(8) to 2.761(6) Å. These hydrogen bonding interactions between the tube-like networks most probably assist in giving 3D order to the structure within the rhombohedral channels and hence the $P4_1$ symmetry of the overall structure.[18] Errors in crystal growth do occur, however, resulting in merohedral twinning.

The shortest M ··· M distances in the structures are across the hydrogen bond bridges between the coordinated water molecules, ranging between 6.450(1) and 6.493(2) Å for **5** and **6**. For **4** the same distances are slightly longer at 6.560(2) and 6.566(2) Å due to the longer Mn–O bonds. Other M ··· M distances are given in Table 3. The shortest M–dca–M distance for each structure is between M(2) and M(4). The shortest internetwork M ··· M distances are slightly less than those across dca bridges, being 7.376(2), 7.288(2) and 7.235(1) Å for **4**, **5** and **6**, respectively.

Co(dca)$_2$(bipy)·0.5H$_2$O·0.5MeOH {7}. Four equatorial dca ligands and two axial bipy ligands are coordinated to each octahedral Co atom in **7**. Each Co is connected to two others by four different bidentate dca ligands coordinating *via* the nitrile nitrogens giving 1D chains of Co(dca)$_2$. These chains are linked together by the bridging bipy ligands resulting in 2D (4,4) sheet networks as shown in Fig. 6. The windows formed by these networks are large enough to allow the bipy ligands of another network to pass through them. Hence the overall structure consists of two sets of parallel 2D sheets interpenetrating at an inclined angle of 61.9°, as shown in Fig. 7. The aromatic rings of each bipy ligand are not coplanar. These ligands stack down the c axis as they alternate from one 2D sheet network to another, with the closest C ··· C interaction between ligands being 3.681(3) Å. The structure was refined with half each of a water and methanol molecule per Co occupying the channels formed

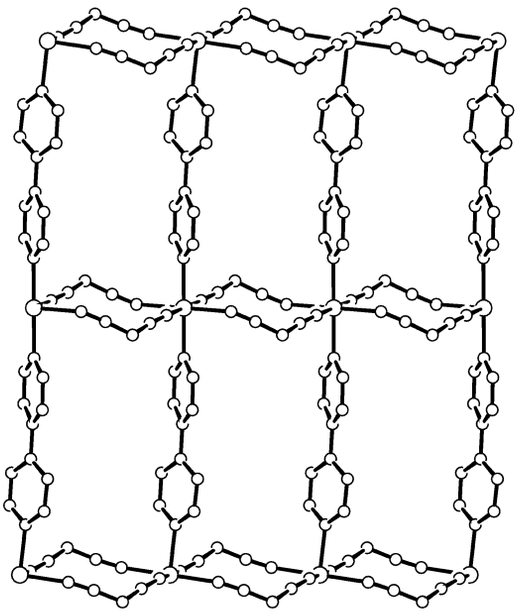

Fig. 6 A (4,4) sheet in the structure of **7**.

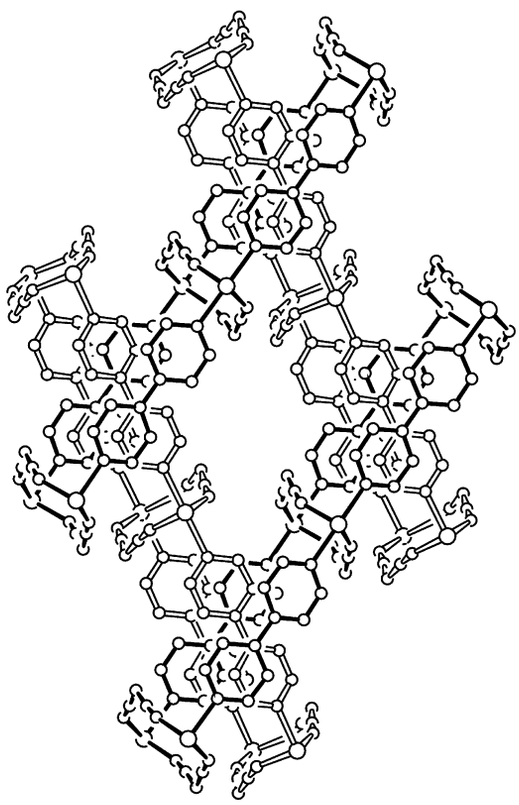

Fig. 7 Four sheets in the structure of **7** showing the inclined interpenetration.

by the interpenetrating sheets. Despite the extreme disorder of the structural solution, hydrogen bonding networks between solvent molecules presumably exist to some extent down the channels. Each dca ligand deflects away from the equatorial plane of the Co atom, due mainly to steric interactions with other dca ligands on adjacent interpenetrating sheets. The $Co–N_{bipy}$ bond length is slightly longer (2.138(2) Å) than the $Co–N_{dca}$ length (av. 2.115 Å). The Co ··· Co separation is 7.349(3) Å across the double dca bridges and 11.3473(2) Å across the bipy bridges. The shortest Co ··· Co distance of 6.8913(2) Å is between adjacent interpenetrating 2D networks.

$Cu(dca)_2(bipy)·H_2O$ {8}. The structure of **8** is similar to that of **7** in that it consists of two sets of parallel 2D sheets interpenetrating at an inclined angle of 65.0°. The Cu atoms are five-coordinate. Each Cu atom is connected to two others by two different dca ligands coordinating through the nitrile nitrogens, giving 1D chains of Cu(dca). As for **7** the 1D chains are linked together by the bridging bipy ligands to give the 2D (4,4) sheet networks. The other dca ligands attached to each Cu atom are monodentate, also coordinating *via* a nitrile nitrogen, and dangle from the same side of each 2D sheet, as shown in Fig. 8.

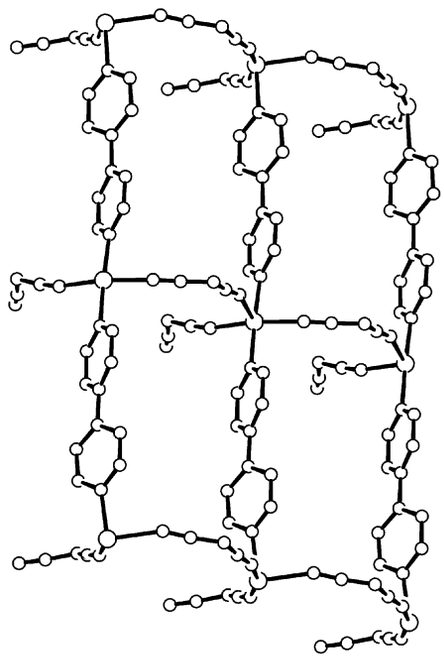

Fig. 8 A (4,4) sheet in the structure of **8**.

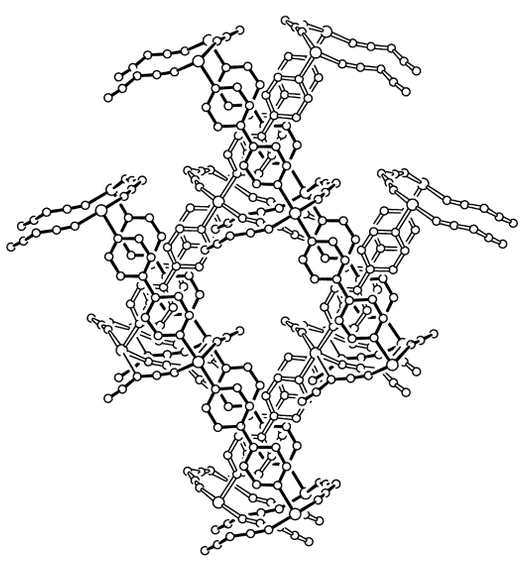

Fig. 9 Four sheets in the structure of **8** showing the inclined interpenetration. The weak intersheet interactions between the amide nitrogen of the monodentate dca ligands and the copper atoms (Cu–N = 2.867(4) Å) are indicated by the thin lines.

Each set of parallel sheets has the monodentate dca ligands on the same side and results in a non-centric structure. The inclined interpenetration[16] of the sheets is shown in Fig. 9. The channels formed by the interpenetrating sheets appear to contain disordered water molecules. These were refined as an oxygen atom disordered over six positions with site occupancy totalling one.

The Cu atoms are distorted square-based pyramidal, but display a weak interaction *trans* to the axial Cu–N(3) bond between the amide nitrogen of the monodentate dca ligand and the Cu atom (2.867(4) Å). This occurs between interpenetrating sheets, cross-linking them into a single, self-penetrating network. The distances between the Cu atoms within the 2D networks are 7.3887(4) and 11.1285(4) Å across the dca and bipy bridges respectively. The shortest Cu ··· Cu separation is again between adjacent 2D networks (6.2499(7) Å), while the closest C ··· C interaction between bipy ligands is 3.495(5) Å.

$Cu(dca)_2(bipy)\cdot MeOH$ {9} and $Cu(dca)_2(bipy)\cdot 2H_2O$ {10}. The structures of **9** and **10** also consist of 2D (4,4) sheet networks. The bridging dca ligands attached to the five-coordinate Cu atoms *via* the nitrile nitrogens give 1D zigzag chains of Cu(dca), rather than the linear arrangement of the Cu atoms observed in **8**. The *trans* bipy ligands link these chains together in a more linear fashion giving the corrugated 2D (4,4) sheet networks. A single monodentate dca ligand is coordinated to each Cu atom *via* a nitrile nitrogen, with these dangling from alternate sides of the corrugated sheets as shown in Fig. 10.

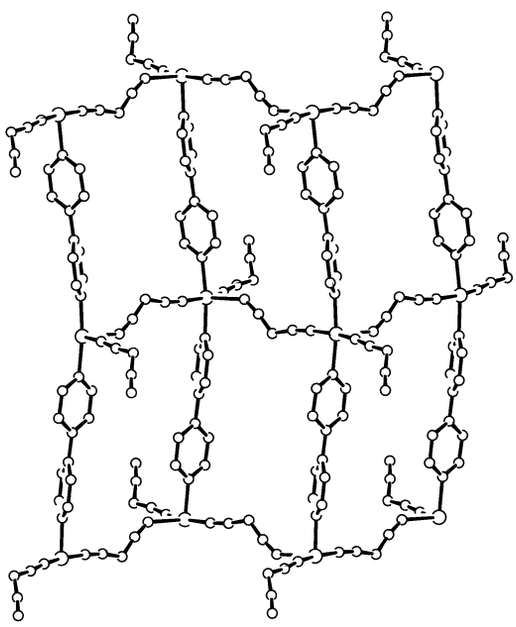

Fig. 10 A (4,4) sheet in the structure of **9**. The structure of **10** is isostructural.

The 2D sheets stack parallel to each other with the dangling dca ligands penetrating the windows of adjacent sheets and hydrogen bonding to solvent molecules *via* the uncoordinated nitriles. These solvent molecules lie in channels formed within the structure. Compounds **9** and **10** are essentially isostructural, with each methanol molecule in **9** replaced by two water molecules in **10**. The two water molecules occupy a little more space, causing changes to the packing of the 2D sheets and resulting in the significant differences in the cell dimensions between **9** and **10** even though the cell volumes are approximately equal.

The coordination geometry around the Cu atoms is again distorted square pyramidal, very similar to that of **8**. In **9** there is also a very weak interaction *trans* to the axial Cu–N(3) bond between the oxygen atom of the methanol and the Cu atom (2.917(2) Å), whereas in **10** the interaction is between one of the two water molecules and the Cu atom, with a distance of 2.925(3) Å.

The lone OH proton in **9** was refined giving a hydrogen bond distance of 2.00(3) Å for H(1) ··· N(6) and an angle of 177(3)° for O(1)–H(1) ··· N(6), while the distance between O(1) and N(6) is 2.906(3) Å. The water protons were not refined in **10**, however there are four unique hydrogen bond distances. Two of these are between the water molecules with O ··· O distances of 2.775(4) and 2.867(3) Å. Another is between one of the water molecules and the uncoordinated nitrile of dca, while the last is between the other water molecule and the amide nitrogen of the bridging dca ligand. These two distances are 2.872(4) and 2.980(4) Å, respectively.

The distances between the Cu atoms within the 2D networks for **9** {**10**} are 8.5848(3) {8.5655(5)} and 11.1109(2) Å {11.0957(6) Å} across the dca and bipy bridges, respectively. The Cu–dca–Cu distance is much longer than that of **8**. The shortest Cu ··· Cu separation is again between adjacent 2D networks: 6.2022(4) Å for **9** and 6.6336(7) Å for **10**.

$Fe(dca)_2(bipy)(H_2O)_2\cdot(bipy)$ {11}. The octahedral Fe atoms in **11** lie on inversion centres and coordinate to two monodentate dca ligands (Fe–N = 2.145(1) Å), two waters (Fe–O = 2.081(1) Å), and two bridging bipy ligands (Fe–N = 2.233(1) Å), the latter giving 1D chains of Fe(bipy). The monodentate dca ligands hydrogen bond to the water molecules on adjacent chains through the uncoordinated nitrile nitrogen and *vice versa*, giving double dca ··· H_2O bridges between the Fe atoms in adjacent chains. These hydrogen bonds extend the 1D coordination network to a 2D (4,4) sheet network, with the 2D sheets packing parallel to each other. Every second sheet in the structure is further connected together by the intercalated bipy ligands which hydrogen bond through the pyridyl nitrogens to the coordinated water molecules. The intercalated bipy molecules penetrate the windows of the other 2D sheets thus giving two 3D interpenetrating α-Po related hydrogen bond networks, as shown in Fig. 11. Each coordinated bipy ligand

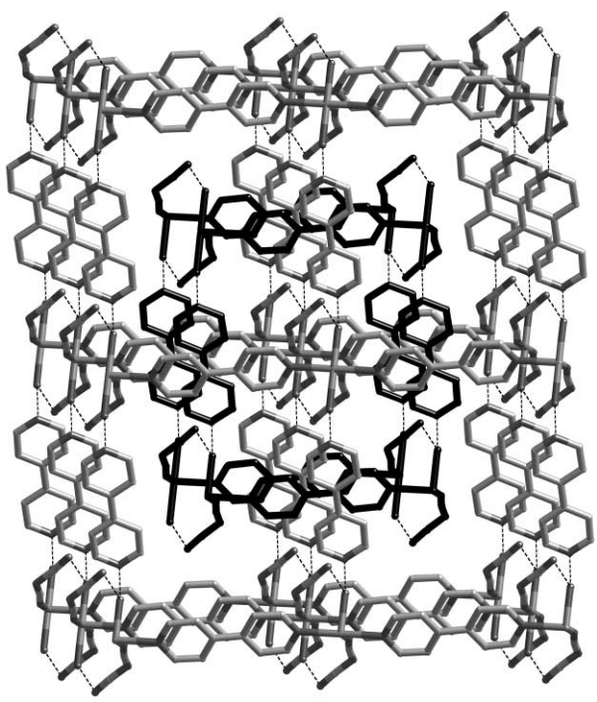

Fig. 11 The two interpenetrating hydrogen bonded networks with α-Po topology in the structure of **11**. Hydrogen bonds are depicted by the dotted lines.

participates in π-stacking with two adjacent intercalated bipy molecules and *vice versa*, giving columns of bipy molecules as viewed down the *a* axis.

Hydrogen bond distances are 1.86(2) and 2.715(2) Å for H-(1) ··· N(5) and O(1) ··· N(5), respectively, between the water and dca ligands, while hydrogen bond distances between the water ligands and intercalated bipy molecules are 1.93(3) and 2.774(2) Å, respectively, for H(2) ··· N(3) and O(1) ··· N(3). The closest C ··· C distance between the π-stacking bipy

Table 4 Magnetic data using a field of 1 T

Complex (M^{II})	μ_{eff}/μ_B (295 K)	θ/K	C/cm^3 mol^{-1} K
1 (Fe)	5.42	−4.2	3.76
2 (Co)	4.84	−18.6	3.15
3 (Ni)	3.07	−2.0	1.17
4 (Mn)	5.78	−1.9	4.20
5 (Fe)	5.44	−4.0	3.75
6 (Co)	5.06	−13.0	3.32
8 (Cu)	1.77	−2.9	0.39
9 (Cu)	1.85	−0.35	0.43

molecules is 3.447(2) Å for C(6) ··· C(10). The shortest Fe ··· Fe distance in the structure is across the double dca ··· H_2O bridges (8.1365(1) Å).

Magnetism

A survey of each system was made by measuring the magnetic moment μ *vs.* temperature over the temperature range 300–2 K in a field of 1 Tesla. Complexes containing metal ions likely to give large anisotropy in susceptibility, *e.g.* Co(II) and Fe(II), were dispersed in Vaseline mulls. This eliminated any temperature dependent crystallite orientation effects. Magnetisation measurements, in field-cooled (5 Oe) and zero-field-cooled modes were made on all samples, in the range 20–2 K, to check for long-range order. The plots were identical, in agreement with a lack of long-range magnetic order. This is as expected in such weakly coupled systems having the long bipy and $\mu_{1,5}$-dca bridging distances. Magnetic moments and Curie–Weiss constants are summarised in Table 4. The plot of moment *versus* temperature is shown for one example, **2**, in Fig. 12.

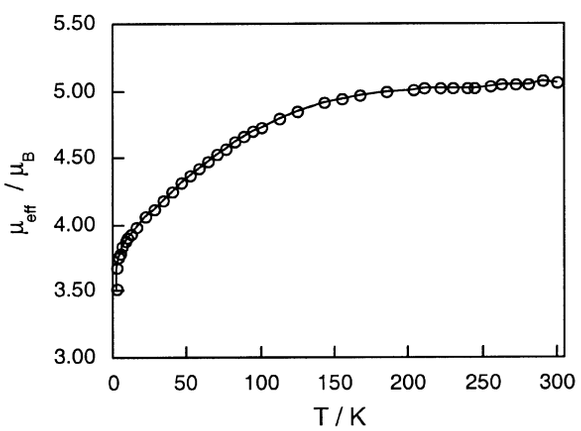

Fig. 12 A plot of effective magnetic moment *versus* temperature in an applied field of 1 T for Co(dca)$_2$(bipy) **2**. The solid line is not a theoretical fit.

The data for **2** are very similar to those of Sun *et al.* reported after completion of our work.[15] The magnetic moments μ_{Co} decrease from a value of 4.84 μ_B at 300 K to reach 3.39 μ_B at 2 K. This is typical behaviour for octahedral Co(II) ($^4T_{1g}$) centres with the temperature dependence arising from a combination of spin–orbit coupling and low symmetry ligand field effects. Very weak antiferromagnetic coupling is also possibly occurring but there is no maximum in the corresponding susceptibilities down to 2 K of the type found at $T_N = 5$ K in the more strongly coupled metamagnetic analogue $CoCl_2$(bipy).[19] It can be seen in Fig. 12 that μ_{Co} values decrease more markedly below approximately 10 K. This region was explored further in variable fields. Thus, at 2 K, and $H = 0$ to 5 T, the magnetisation values almost reach saturation at 5 T with $M = 2.3\ N\beta$, a value much reduced from the $S = 3/2$ value because of spin–orbit and weak coupling effects. Indeed, it is very similar in shape and magnitude to the 2 K isotherms observed for Co(tcm)$_2$[20] and $Ph_4As[Co(dca)_3]$,[21] examples of 3D and 2D networks.

The complex Mn(dca)$_2$(bipy)(H_2O)·0.5H_2O, reported by Manson *et al.*,[13] showed rather similar behaviour to complex **4** with $\theta = -4.7$ K and μ_{Mn} at 300 K of 5.81 μ_B. Use of a Heisenberg chain model for $S = 5/2$ with zero-field splitting assumed zero yielded $J = -0.16$ cm^{-1} in their case. A similar approach for **4** gave $g = 1.96$, $J = -0.104$ cm^{-1}.

The magnetic data for the hydrate–hemimethanolate complexes of Fe(II) and Co(II), **5** and **6**, exhibit very similar behaviour to compounds **1** and **2**, respectively. Preliminary single crystal magnetic measurements were also made on two small crystals (0.650 mg and 0.936 mg) of **6**, a system which has tetragonal symmetry. One single crystal was measured with the longitudinal field parallel to the *a* axis ($\mu_\perp$) while another was measured with the field parallel to the *c* axis ($\mu_{||}$). It was found that $\mu_\perp$ was greater than $\mu_{||}$ between 300 and 4 K. The anisotropy for Co(II) was clearly seen and there is a greater difference between $\mu_\perp$ and $\mu_{||}$ at low temperature (*ca.* 0.6 μ_B). The shape of μ_{Co} *versus* temperature for each crystal orientation is generally similar to that of the bulk sample, which is similar to that of **2** shown in Fig. 12, although neither orientation yields the plateau in μ above 150 K displayed by the powder (dispersed in Vaseline).

The magnetic properties are generally indicative of very weak antiferromagnetic coupling as expected for the long bipy and the $\mu_{1,5}$-NC(N)CN bridging pathways. Consequently, magnetic order is absent in these framework structures, some of which are interpenetrating.

Conclusions

Reaction of first-row transition metals with the ligands 4,4′-bipyridine and dca resulted in a series of eleven new compounds. These materials displayed a larger range of structures in comparison to the related pyrazine series.[3] Topologies displayed were 1D 'tubes', 2D (4,4) sheets (some showing inclined interpenetration), and 3D α-Po nets (showing two-fold interpenetration). Some of these structures showed complicated crystallographic twinning, and pseudopolymorphism was common, with sometimes two or three different products being obtained from the same reaction.

Despite the significant variation in the structures, definitive trends are difficult to assign. In general, however, the structures of the Cu(II) compounds were significantly different to the Mn(II), Fe(II), Co(II) and Ni(II) compounds, due to the ability of Cu(II) to adopt five-coordinate coordination geometry. The next most important structure-determining variable was the solvent mixture, however, as mentioned above, mixtures of different structures were found in the same reactions for a number of the syntheses, and the careful separation of these mixtures was one of the challenges of this work. Some structures also continued to form in spite of solvent mixture variation. This and the fact that the same synthesis can produce at least two very different structures in the one reaction are timely warnings against placing too much emphasis on any 'understanding' of structure formation obtained from the analysis of any of the structures in isolation.

No long-range magnetic order was found in any of the compounds. This is not surprising, given the length of the bipy ligand and the fact that the dca ligands in the structure display only monodentate and $\mu_{1,5}$ bidentate coordination; no tridentate dca coordination, utilising the amide nitrogen atom, was observed. In contrast, 2D (4,4) sheet polymers of type MCl_2(bipy) (M = Fe, Co, Ni) show metamagnetic transitions thought to be due to ferromagnetic coupling along the MCl_2M chains and antiferromagnetic coupling between these chains.[19] The key differences compared to the present weakly coupled species are the short M ··· M distances across the μ-dichloro bridges (3.6 Å) and the favourable superexchange properties of chloro *versus* dicyanamide bridging.

Acknowledgements

This work was supported by grants from the Australian Research Council (ARC Large and Small Grants) to K.S.M. The receipt of an ARC Australian Research Fellowship (to S.R.B.) is gratefully acknowledged.

References and notes

1 (*a*) P. Jensen, S. R. Batten, B. Moubaraki and K. S. Murray, *Chem. Commun.*, 2000, 793; (*b*) S. R. Batten, A. R. Harris, P. Jensen, K. S. Murray and A. Ziebell, *J. Chem. Soc., Dalton Trans.*, 2000, 3829; (*c*) I. Dasna, S. Golhen, L. Ouahab, O. Pena, J. Guillevic and M. Fettouhi, *J. Chem. Soc., Dalton Trans.*, 2000, 129; (*d*) A. Escuer, F. A. Mautner, N. Sanz and R. Vicente, *Inorg. Chem.*, 2000, **39**, 1668; (*e*) G. A. van Albada, M. E. Quiroz-Castro, I. Mutikainen, U. Turpeinen and J. Reedijk, *Inorg. Chim. Acta*, 2000, **298**, 221; (*f*) J. L. Manson, C. D. Incarvito, A. L. Rheingold and J. S. Miller, *J. Chem. Soc., Dalton Trans.*, 1998, 3705; (*g*) S. R. Batten, P. Jensen, B. Moubaraki and K. S. Murray, *Chem. Commun.*, 2000, 2331; (*h*) P. M. van der Werff, S. R. Batten, P. Jensen, B. Moubaraki and K. S. Murray, *Inorg. Chem.*, 2001, **40**, 1718; (*i*) G. A. van Albada, I. Mutikainen, U. Turpeinen and J. Reedijk, *Acta Crystallogr., Sect. E*, 2001, **57**, m421; (*j*) S. R. Marshall, C. D. Incarvito, J. L. Manson, A. L. Rheingold and J. S. Miller, *Inorg. Chem.*, 2000, **39**, 1969; (*k*) A. Claramunt, A. Escuer, F. A. Mautner, N. Sanz and R. Vicente, *J. Chem. Soc., Dalton Trans.*, 2000, 2627; (*l*) I. Riggio, G. A. van Albada, D. D. Ellis, A. L. Spek and J. Reedijk, *J. Inorg. Chim. Acta*, 2001, **313**, 120; (*m*) T. Kusaka, T. Ishida, D. Hashizume, F. Iwasaki and T. Nogami, *Chem. Lett.*, 2000, 1146; (*n*) B.-W. Sun, S. Gao, B.-Q. Ma, D.-Z. Niu and Z.-M. Wang, *J. Chem. Soc., Dalton Trans.*, 2000, 4187; (*o*) B. Jurgens, E. Irran and W. Schnick, *J. Solid State Chem.*, 2001, **157**, 241; (*p*) B.-W. Sun, S. Gao, B.-Q. Ma and Z.-M. Wang, *Inorg. Chem. Commun.*, 2001, **4**, 72; (*q*) B.-W. Sun, S. Gao and Z.-M. Wang, *Chem. Lett.*, 2001, 2; (*r*) J. L. Manson, J. A. Schlueter, U. Geiser, M. B. Stone and D. H. Reich, *Polyhedron*, 2001, **20**, 1423; (*s*) H. Miyasaka, R. Clerac, C. S. Campos-Fernandez and K. R. Dunbar, *Inorg. Chem.*, 2001, **40**, 1663; (*t*) S. Martin, M. G. Barandika, J. I. R. de Larramendi, R. Cortes, M. Font-Bardia, L. Lezama, Z. E. Serna, X. Solans and T. Rojo, *Inorg. Chem.*, 2001, **40**, 3687; (*u*) J. S. Miller and J. L. Manson, *Acc. Chem. Res.*, 2001, **34**, 563; (*v*) J. W. Raebiger, J. L. Manson, R. D. Sommer, U. Geiser, A. L. Rheingold and J. S. Miller, *Inorg. Chem.*, 2001, **40**, 2578; (*w*) S. Martin, M. G. Barandika, R. Cortes, J. I. R. de Larramendi, M. K. Urtiaga, L. Lezama, M. I. Arriortua and T. Rojo, *Eur. J. Inorg. Chem.*, 2001, 2107; (*x*) N. Moliner, A. B. Gaspar, M. C. Munoz, V. Niel, J. Cano and J. A. Real, *Inorg. Chem.*, 2001, **40**, 3986; (*y*) S. Triki, F. Thetiot, J.-R. Galan-Mascaros, J. S. Pala and K. R. Dunbar, *New J. Chem.*, 2001, **25**, 954; (*z*) J. Kohout, L. Jager, M. Hvastijova and J. Kozisek, *J. Coord. Chem.*, 2000, **51**, 169.

2 (*a*) S. R. Batten, P. Jensen, B. Moubaraki, K. S. Murray and R. Robson, *Chem. Commun.*, 1998, 439; (*b*) M. Kurmoo and C. J. Kepert, *New J. Chem.*, 1998, **22**, 1515; (*c*) J. L. Manson, C. R. Kmety, Q. Huang, J. W. Lynn, G. M. Bendele, S. Pagola, P. W. Stephens, L. M. Liable-Sands, A. L. Rheingold, A. J. Epstein and J. S. Miller, *Chem. Mater.*, 1998, **10**, 2552; (*d*) J. L. Manson, C. R. Kmety, A. J. Epstein and J. S. Miller, *Inorg. Chem.*, 1999, **38**, 2552; (*e*) S. R. Batten, P. Jensen, C. J. Kepert, M. Kurmoo, B. Moubaraki, K. S. Murray and D. J. Price, *J. Chem. Soc., Dalton Trans.*, 1999, 2987; (*f*) P. Jensen, S. R. Batten, G. D. Fallon, B. Moubaraki, K. S. Murray and D. J. Price, *Chem Commun.*, 1999, 177; (*g*) K. S. Murray, S. R. Batten, B. Moubaraki, D. J. Price and R. Robson, *Mol. Cryst. Liq. Cryst.*, 1999, **335**, 313; (*h*) C. R. Kmety, Q. Huang, J. W. Lynn, R. W. Erwin, J. L. Manson, S. McCall, J. E. Crow, K. L. Stevenson, J. S. Miller and A. J. Epstein, *Phys. Rev. B*, 2000, **62**, 5576; (*i*) J. L. Manson, C. R. Kmety, F. Palacio, A. J. Epstein and J. S. Miller, *Chem. Mater.*, 2001, **13**, 1068.

3 (*a*) P. Jensen, S. R. Batten, G. D. Fallon, D. C. R. Hockless, B. Moubaraki, K. S. Murray and R. Robson, *J. Solid State Chem.*, 1999, **145**, 387; (*b*) P. Jensen, S. R. Batten, B. Moubaraki, K. S. Murray and R. Robson, *J. Solid State Chem.*, 2001, **159**, 352; (*c*) J. L. Manson, C. D. Incarvito, A. L. Rheingold and J. S. Miller, *J. Chem. Soc., Dalton Trans.*, 1998, 3705; (*d*) J. L. Manson, Q.-Z. Huang, J. W. Lynn, H.-J. Koo, M.-H. Whangbo, R. Bateman, T. Otsuka, N. Wada, D. N. Argyriou and J. S. Miller, *J. Am. Chem. Soc.*, 2001, **123**, 162.

4 P. Jensen, D. J. Price, S. R. Batten, B. Moubaraki and K. S. Murray, *Chem. Eur. J.*, 2000, **6**, 3186.

5 (*a*) C. J. Kepert and M. J. Rosseinsky, *Chem. Commun.*, 1999, 375; (*b*) A. J. Fletcher, E. J. Cussen, T. J. Prior, M. J. Rosseinsky, C. J. Kepert and K. M. Thomas, *J. Am. Chem. Soc.*, 2001, **123**, 10001; (*c*) M. Kondo, T. Yoshitomi, K. Seki, H. Matsuzaka and S. Kitagawa, *Angew. Chem., Int. Ed. Engl.*, 1997, **36**, 1725; (*d*) S. Noro, S. Kitagawa, M. Kondo and K. Seki, *Angew. Chem., Int. Ed.*, 2000, **39**, 2082; (*e*) O. M. Yaghi and H. Li, *J. Am. Chem. Soc.*, 1995, **117**, 10401; (*f*) O. M. Yaghi and H. Li, *J. Am. Chem. Soc.*, 1996, **118**, 295.

6 (*a*) R. Hooft, COLLECT Software, Nonius BV, Delft, The Netherlands, 1998; Z. Otwinowski and W. Minor, in *Methods in Enzymology*, ed. C. W. Carter and R. M. Sweet, Academic Press, New York, 1996.

7 XPREP, version 5.03, Siemens Analytical X-ray Instruments Inc., Madison, Wisconsin, USA, 1994.

8 S. Mackay, C. J. Gilmore, C. Edwards, M. Tremayne, N. Stewart and K. Shankland, maXus: a computer program for the solution and refinement of crystal structures from diffraction data, University of Glasgow, Scotland, UK, Nonius BV, Delft, The Netherlands, MacScience Co. Ltd., Yokohama, Japan, 1998.

9 teXsan: Single Crystal Structure Analysis Software, version 1.6, Molecular Structure Corporation, The Woodlands, TX. 1993.

10 G. M. Sheldrick, SHELX-97, Program for crystal structure refinement, University of Göttingen, Göttingen, Germany, 1997.

11 D. C. Palmer, CrystalDiffract 2.1.0, CrystalMaker Software, Bicester, UK, 1999.

12 T. J. B. Holland and S. A. T. Redfern, *Mineral. Mag.*, 1997, **61**, 65.

13 (*a*) J. L. Manson, C. D. Incarvito, A. M. Arif, A. L. Rheingold and J. S. Miller, *Mol. Cryst. Liq. Cryst.*, 1999, **334**, 605; (*b*) J. L. Manson, A. M. Arif, C. D. Incarvito, L. M. Liable-Sands, A. L. Rheingold and J. S. Miller, *J. Solid State Chem.*, 1999, **145**, 369.

14 The formation of different structures from similar or even identical reagents is well known for coordination polymers – see, for example, (*a*) refs. 1*b*, 2*f*, 3; (*b*) S. R. Batten and K. S. Murray, *Aust. J. Chem.*, 2001, **54**, 605; (*c*) C. Janiak, L. Uehlin, H.-P. Wu, P. Klufers, H. Piotrowski and T. G. Scharmann, *J. Chem. Soc., Dalton Trans.*, 1999, 3121; (*d*) H.-P. Wu, C. Janiak, Rheinwald and H. Lang, *J. Chem. Soc., Dalton Trans.*, 1999, 183; (*e*) C. Janiak and H. Hemling, *J. Chem. Soc., Dalton Trans.*, 1994, 2947; (*f*) C. Janiak, S. Temizdemir, T. G. Scharmann, A. Schmalstieg and J. Demtschuk, *Z. Anorg. Allg. Chem.*, 2000, **626**, 2053.

15 B.-W. Sun, S. Gao, B.-Q. Ma and Z.-M. Wang, *New J. Chem.*, 2000, **24**, 953.

16 S. R. Batten and R. Robson, *Angew. Chem., Int. Ed.*, 1998, **37**, 1460.

17 S. R. Batten, P. Jensen, B. Moubaraki and K. S. Murray, *Chem. Commun.*, 2000, 2331.

18 The importance of hydrogen bonding solvent molecules in determining structure design has been examined in C. Janiak, T. G. Scharmann, W. Gunther, F. Girgsdies, H. Hemling, W. Hinrichs and D. Lentz, *Chem. Eur. J.*, 1995, **1**, 637.

19 M. A. Lawandy, X. Huang, R.-J. Wang, J. Li, J. Y. Lu, T. Yuen and C. L. Lin, *Inorg. Chem.*, 1999, **38**, 5410.

20 S. R. Batten, B. F. Hoskins, B. Moubaraki, K. S. Murray and R. Robson, *J. Chem. Soc., Dalton Trans.*, 1999, 2977.

21 P. M. van der Werff, S. R. Batten, P. Jensen, B. Moubaraki, K. S. Murray and E. H.-K. Tan, *Polyhedron*, 2001, **20**, 1129.